weighing. The 22 hydrogen atoms were included in the final cycles of refinement and held at idealized geometry. Final cycles included $1/\Sigma^{25}$ weighting scheme and converged at $R_1 = 0.053$ and $R_w = 0.068$ for the 1481 reflections, with an estimated standard deviation of an observation of unit weight of 1.970. In the final cycle of least-squares refinement, no shift/error was greater than 0.07 averaging less than 0.01.

Acknowledgment. We acknowledge Louis Agnew, Dr. Laddawan Borsub, and James Most for synthetic help and also Jackie Benke, Ellie Burke, and Dr. Asirur Rahman for technical assistance. We especially thank Dr. Jane Griffen, Medical Foundation of Buffalo Inc., Research Labs, Buffalo, NY, for an X-ray data search on organogermanium compounds. The Eagle-Picher Chemical Co. provided a generous gift of di-*n*-butyldichlorogermane. High-resolution mass spectrometry was performed by the Midwest Center for Mass Spectrometry, an NSF regional instrumentation facility. A.G.S. thanks Marquette University for a research fellowship.

(25) Hahn, T. *International Tables for Crystallography*; Riedel: Dordrect, Holland, 1983; Vol. A.

Registry No. **1**, 876-05-1; **2**, 39590-04-0; **3**, 3965-56-8; **4**, 55606-07-0; **5**, 58066-43-6; **6**, 126696-64-8; **7**, 126696-65-9; **8a**, 126696-66-0; **8b**, 126696-74-0; **9a**, 126696-67-1; **9b**, 126696-75-1; **10a**, 126696-68-2; **10b**, 126696-76-2; **11a**, 126696-69-3; **11b**, 126696-77-3; **12**, 80864-33-1; **13**, 126696-70-6; **14**, 126696-71-7; **15**, 126696-72-8; **16**, 126696-73-9; norbornene, 498-66-8; *trans*-1,3-bis(((*p*-tolylsulfonyl)oxy)methyl)cyclopentane, 70723-29-4; dichlorodiphenylgermane, 1613-66-7; dichlorodimethylgermane, 1529-48-2; di-*n*-butyldichlorogermane, 4593-81-1.

Supplementary Material Available: A list of anisotropic thermal parameters for **6** (1 page); a structure factor table (13 pages). Ordering information is given on any current masthead page. A diagram of the "slow drop" adaptor is also available on direct request to the authors.

Investigation of the Electrochemical Behavior and Electronic Structure of (μ-Butatriene)hexacarbonyldiiron Complexes

Domenico Osella,* Olimpia Gambino, and Roberto Gobetto

Dipartimento di Chimica Inorganica, Chimica Fisica e Chimica dei Materiali, Università di Torino, Via P. Giuria 7, 10125 Torino, Italy

Piero Zanello* and Franco Laschi

Dipartimento di Chimica, Università di Siena, Siena, Italy

Catherine E. Housecroft* and Steven M. Owen

University Chemical Laboratory, Cambridge, U.K.

Received September 11, 1989

The redox chemistry of (μ-butatriene)hexacarbonyldiiron compounds, $Fe_2(CO)_6(RR'C{=}C{=}C{=}CRR')$, has been investigated by electrochemical and spectroscopic methods and Fenske–Hall quantum-chemical calculations. The sequence of the electrode processes has been postulated on the basis of the response of different electrochemical techniques, electron spin resonance (ESR) spectroscopy, and chemical tests. The butatriene chain, interacting with the bimetallic $Fe_2(CO)_6$ framework in a multicentered σ/π fashion, is able to stabilize the electrogenerated anions.

Introduction

A number of stable (cumulene)hexacarbonyldiiron compounds have been reported.[1] These complexes show that the $Fe_2(CO)_6$ frame is able to stabilize through extensive σ/π coordination even the unsubstituted butatriene $H_2C{=}C{=}C{=}CH_2$, which is not isolable under usual conditions.[2]

The butatriene complexes can be synthesized by starting from iron carbonyls (i.e. $Fe(CO)_5$, $Fe_2(CO)_9$, and $Fe_3(CO)_{12}$) according to the following methods: (a) reaction with stable cumulene,[2] (b) zinc-assisted dehalogenation of alkynyl dihalides,[2] and (c) dehydroxylation of alkynediols.[3] Since these compounds are diamagnetic, the EAN formalism requires the interaction of all six π-electrons of the butatriene chain and the presence of an iron–iron bond.

Two X-ray structural determinations have been reported for $Fe_2(CO)_6$[μ-bis(biphenylylene)butatriene][4] and $Fe_2(CO)_5(PPh_3)$(μ-butatriene)[5] molecules. The butatriene chain assumes a nonlinear configuration twisted end by end by about 90°. This modification of the originally linear butatriene is dictated by the optimum overlap of the cumulene π MO's with the iron AO's. These structural descriptions have been corroborated by a ^1H NMR study in a nematic phase[6] and by a ^{13}C NMR investigation of a large number of such derivatives.[7] Finally, quantum-mechanical calculations within the CNDO scheme on some butatriene complexes[8] coupled with an UV-PES study have been performed.

(1) Nakamura, A. *Bull. Chem. Soc. Jpn.* **1965**, *38*, 1868. Nakamura, A.; Kim, P.-J.; Hagihara, N. *J. Organomet. Chem.* **1966**, *6*, 420. Joshi, K. K. *J. Chem. Soc. A* **1966**, 594. Joshi, K. K. *Ibid.* **1966**, 598. King, R. B. *J. Am. Chem. Soc.* **1966**, *88*, 2075.
(2) Nakamura, A.; Kim, P.-J.; Hagihara, N. *J. Organomet. Chem.* **1965**, *3*, 7.
(3) Victor, R. *J. Organomet. Chem.* **1977**, *127*, C25.
(4) Bright, D.; Mills, O. S. *J. Chem. Soc., Dalton Trans.* **1972**, 2465.
(5) Gerlach, J. N.; Wing, R. M.; Ellgen, P. C. *Inorg. Chem.* **1976**, *15*, 2959.
(6) Arumngam, S.; Kunwar, A. C.; Khetrapalm, C. C. *J. Organomet. Chem.* **1984**, *265*, 73.
(7) Victor, R.; Riugel, I. *Org. Magn. Reson.* **1978**, *11*, 31.
(8) Granozzi, G.; Casarin, M.; Aime, S.; Osella, D. *Inorg. Chem.* **1982**, *21*, 4073.

0276-7333/90/2309-1792$02.50/0

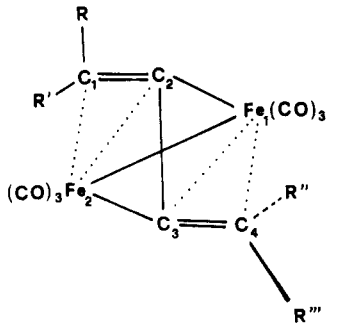

Figure 1. Sketch of the structure of the μ-butatriene complexes under study along with the atom-numbering scheme employed in the Fenske–Hall calculations: R = R′ = R″ = R‴ = H, **1**; R = R‴ = Me, R′ = R″ = H, **2a**; R′ = R‴ = Me, R = R″ = H, **2b**; R′ = R″ = Me, R = R‴ = H, **2c**; R = R′ = R″ = R‴ = Me, **3**; R = R′ = R″ = R‴ = Ph, **4**.

In some of these investigations, it has been suggested that the description of such molecules requires two valence-bond formulas. In the former the organic chain is viewed as a *trans*-butadiene σ-bonded via the central carbon atoms and π-bonded via the terminal double bonds (Figure 1); in the latter the chain is regarded as a bis-(η^3-allyl) system. These features prompted us to undertake an electrochemical investigation of a number of such compounds coupled with theoretical calculations within the Fenske–Hall scheme. In particular, we are interested in understanding whether the butatriene chain is able to stabilize the electrogenerated anions by clasping the $Fe_2(CO)_6$ moiety together.

Results and Discussion

Electrochemical Investigation. The butatriene complexes **1–4** have been synthesized by reacting $Fe_3(CO)_{12}$ with the appropriate alkynediol in acetone.[3] Their purity has been checked by IR and ^1H and ^{13}C NMR spectroscopy.

According to a previous report,[7] complex **2**, namely $Fe_2(CO)_6$(MeHC=C=C=CHMe), has been obtained as an isomeric mixture, where isomer **2a** (having the two methyl groups trans to carbon atoms) is by far the most abundant one (Figure 1).

The CV response of **2** is similar to those of isomeric pure **1**, **3**, and **4** complexes and shows no spurious peaks. The different isomers probably exhibit very close reduction waves, which completely overlap in the cyclic voltammogram. As shown in Figure 2, complex **1** undergoes a single-step reduction process, whereas the other butatriene complexes **2–4** undergo two distinct reduction steps at a mercury electrode in acetonitrile solution.

In each case, controlled-potential coulometry at potentials 100 mV beyond the wave in **1**, or the more cathodic wave in **2–4**, indicates that the overall reduction consumes 2 faradays/mol. For the unsubstituted $Fe_2(CO)_6(H_2C{=}C{=}C{=}CH_2)$ derivative (**1**), the reduction proceeds through an apparently single-step two-electron process, which is totally irreversible. In fact, even at a scan rate as high as 10.0 V s^{-1}, no directly associated reoxidation wave can be detected.

A rotating-disk-electrode (RDE) test on an acetonitrile solution of **1** at a mercury-plated gold electrode (f' = 800 rpm, scan rate 5 mV s^{-1}) shows a linear plot of E vs log $[(i_l - i)/i]$ with a 33-mV slope consistent with a two-electron quasi-reversible (diffusion-controlled) process. Thus, the overall irreversibility is associated with a fast chemical decomposition of the electrogenerated dianion 1^{2-}, as confirmed by the presence of several small reoxidation waves in the CV reverse scan, rather than with an intrinsically slow electron-transfer rate.

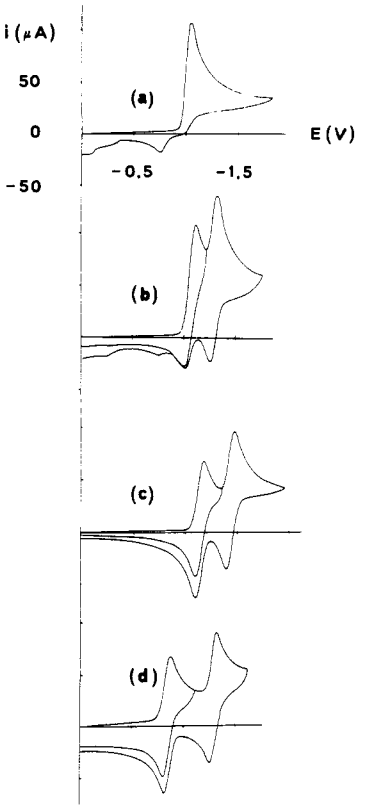

Figure 2. Cyclic voltammograms recorded at a mercury electrode on acetonitrile solutions containing $[NEt_4][ClO_4]$ (0.1 mol dm^{-3}) and (a) **1** (1.2 mmol dm^{-3}), (b) **2** (1.1 mmol dm^{-3}), (c) **3** (1.7 mmol dm^{-3}), or (d) **4** (1.0 mmol dm^{-3}). Scan rate 0.2 V s^{-1}.

In contrast, the substituted derivatives **2–4** exhibit two distinct one-electron reductions. However, marked differences are found in the separation of the formal electrode potentials of the two subsequent reductions as well as in the stabilities of the electrogenerated mono- and dianions.

In the case of $Fe_2(CO)_6$(MeHC=C=C=CHMe) (**2**), analysis[9,10] of the first reduction response, 0/1−, with scan rate shows that the current ratio between the cathodic wave and its directly associated anodic wave (i_p^a/i_p^c) is practically zero at 0.02 V s^{-1} and gradually increases up to unity at 2.0 V s^{-1}. This indicates that the 0/1− redox process is followed by chemical decomposition of the monoanion 2^-. Assuming a first-order chemical reaction, we can calculate a half-life of about 2 s for the monoanion 2^-. A fairly shorter half-life can be associated with the dianion 2^{2-}.

In contrast, the reduction processes for **3** and **4** afford stable mono- and dianions, at least on the CV time scale. Indeed, for the two complexes the i_p^a/i_p^c ratio is constantly equal to unity for 0/1− and 1−/2− redox processes.

The difference between the peak potential of the forward and backward responses, $\Delta E_p = E_p^c - E_p^a$, gradually increases from 70 (at 0.02 V s^{-1}) to 200 mV (at 5.0 V s^{-1}) for 0/1− and from 90 to 320 mV for 1−/2− processes in the same scan rate range. Under the same experimental conditions, the oxidation of ferrocene, which is assumed to be a "perfectly" reversible electron transfer, actually exhibits at a Pt electrode an increase of ΔE_p from 65 to 120 mV. Therefore, we can state that complexes **3** and **4**

(9) Brown, E. R.; Sandifer, J. R. In *Physical Methods of Chemistry: Electrochemical Methods*; Rossiter, B. W., Hamilton, J. F., Eds.; Wiley: New York, 1986; Vol. 2.
(10) Bard, A. J.; Faulkner, L. R. *Electrochemical Methods*; Wiley: New York, 1980.

Table I. Formal Electrode Potentials (in V vs SCE) of the Diiron Complexes 1–4

	CH_3CN			CH_2Cl_2	
complex	$E^{\circ\prime}_{0/1-}$	$E^{\circ\prime}_{1-/2-}$	$E_p{}^a{}_{3/2+}$	$E^{\circ\prime}_{0/1-}$	$E^{\circ\prime}_{1-/2-}$
$Fe_2(CO)_6(C_4H_4)$ (1)	−1.08[a]	−1.08[a]	+1.39	−1.32[a]	−1.32[a]
$Fe_2(CO)_6(C_4H_2Me_2)$ (2)	−1.06	−1.29	+1.41	−1.19	−1.40
$Fe_2(CO)_6(C_4Me_4)$ (3)	−1.13	−1.42	+1.05	−1.22	−1.45
$Fe_2(CO)_6(C_4Ph_4)$ (4)	−0.83	−1.31	+1.08	−0.94	−1.36

[a] Single two-electron wave.

undergo two subsequent *quasi*-reversible one-electron reductions uncomplicated by following chemical reactions. The ΔE_p values for both complexes suggest that the heterogeneous charge transfers are somewhat slower for the 1−/2− with respect to the relative 0/1− processes: Corroboration for this hyphothesis comes from a RDE test on an acetonitrile solution of **3** at a mercury-plated electrode (f' = 800 rpm, scan rate 5 mV s^{-1}). Two well-resolved waves are observed, characterized by almost equal limiting currents ($i_l(0/1-)$ = 87 μA, $i_l(1-/2-)$ = 82 μA).

The 0/1− wave exhibits a $E_{3/4} - E_{1/4}$ value of 60 mV and a slope of the linear plot of E vs log $[(i_l - i)/i]$ equal to 62 mV. The 1−/2− wave shows a $E_{3/4} - E_{1/4}$ value of 85 mV and a slope of the linear plot of E vs log $[(i_l - i)/i]$ equal to 88 mV.

According to the generally accepted electrochemical criteria,[9,10] these features indicate a more pronounced kinetic sluggishness for the second electron transfer. Thus, one can speculate that the 1−/2− process is accompanied by a somewhat significant structural rearrangement of the complex[11] (vide infra).

The same overall electrochemical features hold in the less coordinating dichloromethane solvent. Table I summarizes the redox potentials of the butatriene complexes. As one goes from a mercury to a platinum working electrode, the rate of the heterogeneous charge transfer slows down for all complexes; this, however, leaves substantially unaltered the formal electrode potentials, $E^{\circ\prime} \simeq E_{1/2} = (E_p{}^c + E_p{}^a)/2$. Such a behavior is not unusual in organometallic electrochemistry; i.e., Hg is not an "innocent" electrode material but could stabilize the electrogenerated anions.[12]

The use of a platinum electrode provides evidence that in acetonitrile solvent (where the anodic range is wider) a totally irreversible two-electron oxidation process also occurs for all the compounds under study (Table I). The depopulation of the HOMO, which represents the iron–iron interaction (vide infra), causes a quick and irreversible decomposition of the butatriene complexes.

Interestingly, the difference between the formal electrode potentials of the two subsequent reductions, $\Delta E^{\circ\prime} = E^{\circ\prime}(0/1-) - E^{\circ\prime}(1-/2-)$, increases as the number and the steric bulk of the substituents of the butatriene chain increases. In fact, $\Delta E^{\circ\prime}$ is <150 mV for **1** (i.e. the two reduction processes are actually indistinguishable in the CV experiment)[13] and 230, 290, and 480 mV for **2**–**4**, respectively. Coulombic effects should make $E^{\circ\prime}(1-/2-)$ more negative with respect to $E^{\circ\prime}(0/1-)$. For instance, the two subsequent reductions of several aromatic hydrocarbons, where the two electrons add to the same nondegenerate LUMO, show a $\Delta E^{\circ\prime}$ value of 700 mV.[14] This represents, to a first approximation, the energy required

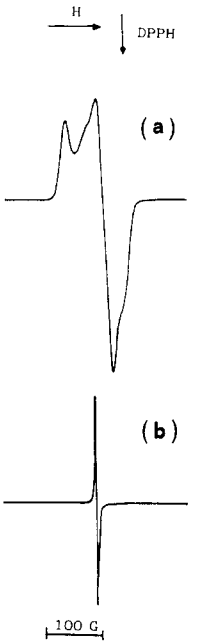

Figure 3. X-Band ESR spectra of 3^- electrogenerated at a mercury pool (E_w = −1.30 V) from a CH_2Cl_2 solution containing **3** (6.7 mmol dm^{-3}) and $[NBu_4][ClO_4]$ (0.2 mol dm^{-3}): (a) liquid-nitrogen-temperature; (b) ambient temperature.

to overcome electronic repulsion within the same orbital. Several organometallic clusters exhibit similar features and, accordingly, the $\Delta E^{\circ\prime}$ values are almost independent of chain substituents and metal composition.[15] In contrast, lower $\Delta E^{\circ\prime}$ values can be found when structural changes accompany the charge transfer, making more facile the second reduction step. This is the case for $Cr(CO)_3$(arene)[16] and $Fe_3(CO)_9$(alkyne)[17] compounds.

The Fenske–Hall calculations (vide infra) clearly indicate the presence of a nondegenerate LUMO having, moreover, negligible contributions from the butatriene MO's, which rules out any important conjugation effects through the organic chain. A possible explanation of these data is that the 1−/2− reduction of the butatriene complexes is likely to be accompanied by a structural rearrangement of the organic chain. This structural change facilitates the second reduction step, thereby decreasing the value of $\Delta E^{\circ\prime}$. As the steric bulk of the chain substituents increases, structural reorganization is hindered and the reduction to the dianion is less favorable.

ESR Study of Electrogenerated Anions. As expected from its CV response, the monoanion 2^- is very labile. An isotropic ESR signal can be detected immediately after the exhaustive one-electron reduction of **2** in acetonitrile solution at a mercury pool (Table II). This signal rapidly vanishes while new, small resonances from unidentified paramagnetic fragments begin to appear. In contrast, complexes **3** and **4** give stable monoanions. Figure 3 shows the liquid-nitrogen-temperature (a) and the room-temperature (b) X-band EPR spectra of 3^-, electrogenerated in dichloromethane solution. The spectrum of the frozen solution is indicative of a rhombic structure (g_l = 2.068; g_m = 2.025; g_h = 2.007). The room-temperature g_{iso} value of 2.032 (ΔH_{iso} = 5.4 G) agrees nicely with the calculated g_{iso} value of 2.033. The line shape analysis of the spectra

(11) Geiger, W. E. *Prog. Inorg. Chem.* **1985**, *33*, 275.
(12) Bond, A. M.; Peake, B. M.; Robinson, B. H.; Simpson, J.; Watson, D. J. *Inorg. Chem.* **1977**, *16*, 419. Brockway, D. J.; West, B. O.; Bond, A. M. *J. Chem. Soc., Dalton Trans.* **1979**, 1891.
(13) Heinze, J. *Angew. Chem., Int. Ed. Engl.* **1984**, *23*, 831.
(14) McKinney, T. H. *Electroanal. Chem.* **1980**, *10*, 97.
(15) Lindsay, P. M.; Peake, B. M.; Robinson, B. H.; Simpson, J.; Howrath, H.; Vahrenkamp, H.; Bond, A. M. *Organometallics* **1984**, *3*, 413.
(16) Rieke, R. D.; Arney, J. S.; Rich, W. E.; Willeford, B. R.; Poliner, B. S. *J. Am. Chem. Soc.* **1979**, *97*, 5951.
(17) Osella, D.; Gobetto, R.; Montangero, P.; Zanello, P.; Cinquantini, A. *Organometallics* **1986**, *5*, 1247.

Table II. X-Band EPR Parameters of the Monoanions 2^-–4^- Electrogenerated in Different Solvents

	CH_2Cl_2					MeCN				
monoanion	g_1	g_m	g_h	g_{iso}	ΔH_{is3}/G	g	g_m	g_h	g_{iso}	ΔH_{iso}/G
2^-	...	...	...			...		...	2.042	5.5
3^-	2.068	2.025	2.007	2.032	5.4	2.065	2.032	*a*	2.035	5.5
4^-	2.066	2.025	2.004	2.031	4.0	2.067	2.027	2.003	2.032	5.3

[a] The line broadening arising from acetonitrile solvent prevents an accurate evaluation of this parameter.

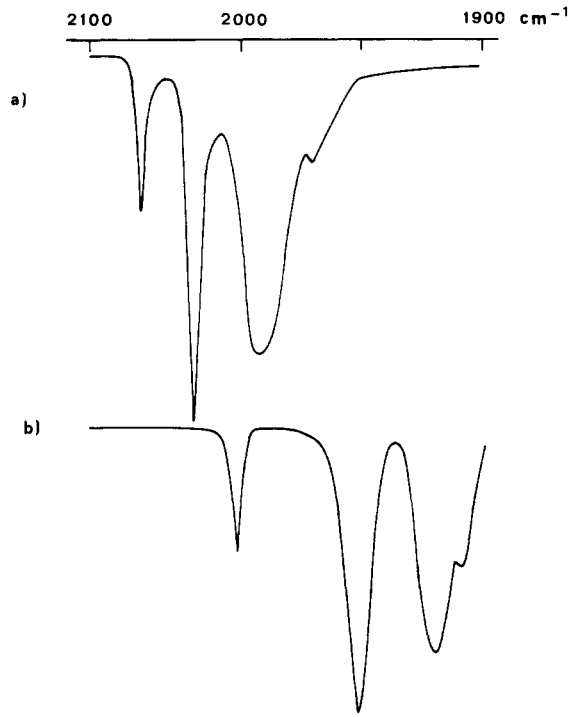

Figure 4. IR spectra in the CO stretching region of a CH_2Cl_2 solution of **3** (a) before and (b) after one-electron electrolysis at a mercury pool (E_w = −1.30 V): **3**, 2063 m, 2021 vs, 1987 s, br, 1968 m, sh cm^{-1}; 3^-, 2000 m, 1950 vs, 1920 s, br, 1907 m, sh cm^{-1}.

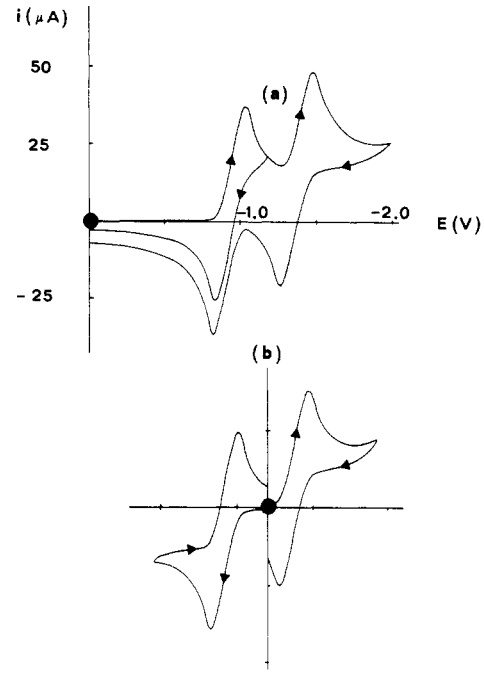

Figure 5. Cyclic voltammograms recorded at a platinum electrode on a dichloromethane solution containing **4** (2.3 mmol dm^{-3}) and $[NBu_4][ClO_4]$ (0.1 mol dm^{-3}) (● marks the initial scan): (a) starting solution; (b) solution after one-electron reduction at a mercury-pool electrode (E_w = −1.06 V). Scan rate 20 mV s^{-1}.

of 3^- in both dichloromethane and acetonitrile and in the temperature range from 100 to 300 K does not reveal any hyperfine splitting, thus suggesting the fact that the added electron does not reside on the organic chain, according to the metallic character of the LUMO (vide infra).

The ESR rhombic pattern along with the near-reversibility of the 0/1− electron transfer suggests that anion 3^- has a geometry similar to that of parent complex **3**. Indeed, IR spectra, recorded before and after one-electron exhaustive electrolysis in acetonitrile, exhibit very similar patterns in the ν_{CO} stretching region for **3** and 3^-, the latter being shifted uniformly about 60 cm^{-1} (Figure 4). This is in accord with a significant charge delocalization onto the $Fe_2(CO)_6$ moiety.[18] Analogous ESR and IR patterns are displayed by 4^- (Table II). Evidence of the stability of monoanions 3^- and 4^- is also given by CV tests performed on electrolyzed solutions of **3** and **4**. As an example, in Figure 5 the CV response of **4** in dichloromethane solution (a) is compared with that recorded after its exhaustive one-electron reduction at −1.06 V (b). It is easy to see that the two responses are complementary, indicating the persistence of the monoanion 4^-.

Macroelectrolyses at potentials corresponding to the second reduction steps reveal that 2^{2-} is highly unstable. In addition 3^{2-} and 4^{2-}, which appeared to be stable on the shorter CV time scale, are in fact similarly unstable. As a common feature, the increasing consumption of charge

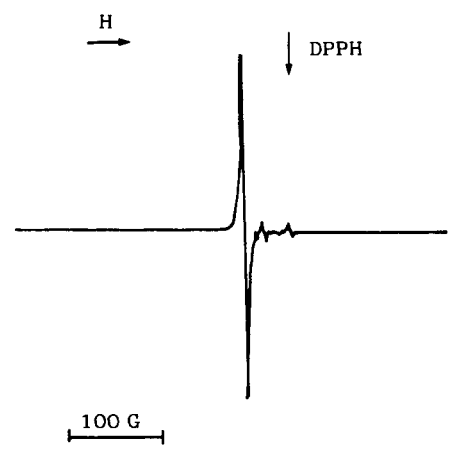

Figure 6. Ambient-temperature ESR spectrum recorded on an acetonitrile solution of **4** (2.2 mmol dm^{-3}) and $[NEt_4][ClO_4]$ (0.1 mol dm^{-3}) after the consumption of 1.5 e/molecule at a mercury-pool electrode (E_w = −1.40 V).

passing from 1 to 2 faradays/mol corresponds in the ESR spectrum to a decrease in intensity of the resonance of the monoanion and to the appearance of new, small signals that are assigned to paramagnetic fragments. In Figure 6 the ESR spectrum of an acetonitrile solution of **4** after 1.5 faradays/mol is reported.

Chemical tests confirm the instability of electrogenerated dianions. After exhaustive two-electron electrolyses of **3** and **4**, electrochemical reoxidation at 0.00 V vs SCE or chemical reoxidation with an excess of $AgPF_6$ does not

(18) Connor, R. E.; Nicholas, K. M. *J. Organomet. Chem.* **1977**, *123*, C45.

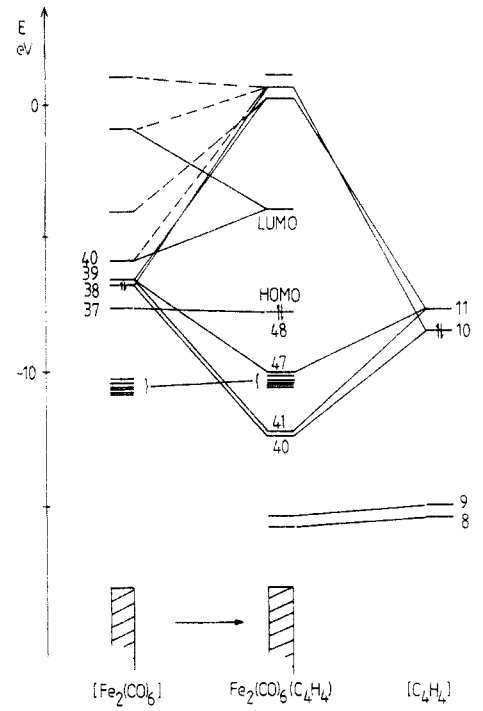

Figure 7. Correlation of the molecular orbitals of the $Fe_2(CO)_6$ and $H_2C{=}C{=}C{=}CH_2$ fragments in 1. Fragment orbital energies are taken from the Fock matrix of complex 1. A dotted correlation line indicates that a metal fragment MO mixes into an MO of 1 but does not overlap significantly with an MO of the butatriene fragment.

afford any identifiable organometallic compounds. In contrast, the same procedure after one-electron electrolysis gives back the parent complexes in almost quantitative yields.

MO Calculations. The bonding in 1 has been considered in terms of the interaction of an $Fe_2(CO)_6$ fragment with butatriene, $H_2C{=}C{=}C{=}CH_2$, and the results compare favorably with those obtained by using the CNDO methods.[8] The drawings at the top of Figure 8 illustrate the orientation of the butatriene molecule relative to the $Fe_2(CO)_6$ framework, and a correlation diagram for the interaction of the MO's of the two fragments is given in Figure 7. The frontier orbitals of the $Fe_2(CO)_6$ fragment have been previously described,[19] and it is important to remember that the directionality of the orbitals is significantly affected by the orientation of the carbonyl ligands.[19] Thus, for example, although MO 37 (Figure 8a) possesses Fe–Fe bonding character, the electron density is concentrated on the side of the metal–metal bond away from the butatriene ligand. This is a direct consequence of the disposition of the carbonyl ligands, and as a result, interaction of MO 37 with the butatriene orbitals is negligible; MO 37 becomes the HOMO of 1 (Figure 7), as was noted in the previous CNDO results.[8] The primary interfragment interactions involve MO's 38 and 39 of $Fe_2(CO)_6$ and MO's 10 and 11 of $H_2C{=}C{=}C{=}CH_2$; the orbital interactions (39–11) and (38–10) are schematically illustrated in Figure 8b,c. The twisted nature of the organic chain (see insert in Figure 8) provides the carbon π-system with the versatility it requires to allow each of MO's 11 and 10 to simultaneously, and efficiently, overlap with the $Fe_2(CO)_6$ fragment MO's 39 and 38, respectively.

The results of the Fenske–Hall calculations support those drawn from earlier CNDO calculations[8] (see the

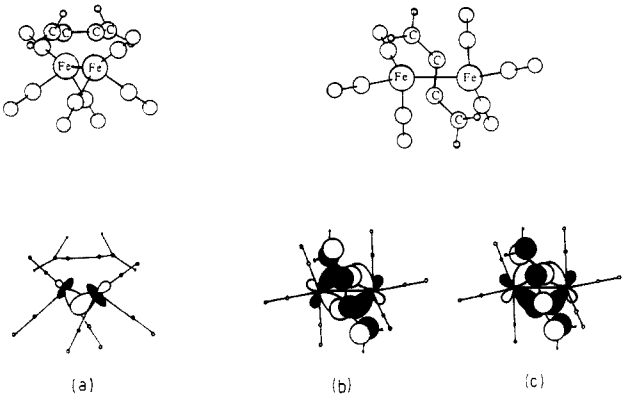

Figure 8. Schematic representations of (a) MO 37 of the $Fe_2(CO)_6$ fragment, which becomes the HOMO of 1, (b) the interaction of $Fe_2(CO)_6$ MO 39 and $H_2C{=}C{=}C{=}CH_2$ MO 11, and (c) the interaction of $Fe_2(CO)_6$ MO 38 and $H_2C{=}C{=}C{=}CH_2$ MO 10.

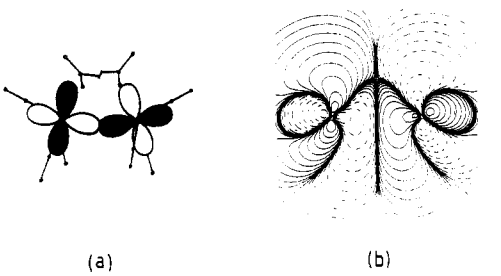

Figure 9. The LUMO of 1: (a) schematic representation; (b) amplitude contour plot in the plane containing the Fe–Fe bond and bisecting the butadiene ligand through C(2)–C(3).

Table III. Interatomic Mulliken Overlap Populations in 1[a]

bond	Mulliken overlap population/e	
	Fenske–Hall[b]	CNDO[c]
Fe(1)–C(2) = Fe(2)–C(3)	0.14	0.22
Fe(1)–C(3) = Fe(2)–C(2)	−0.05	0.00
Fe(1)–C(4) = Fe(2)–C(1)	0.03	0.07
C(1)–C(2) = C(3)–C(4)	0.61	1.07
C(2)–C(3)	0.68	1.38

[a] Atom numbering is given in Figure 1. [b] This work. [c] Reference 8.

interatomic Mulliken overlap populations in Table III). Both sets of results point out that the *trans*-butadiene valence-bond formula (Figure 1) is the most appropriate.

Reduction of complex 1 should result in a lengthening of the Fe–Fe bond since the LUMO (well separated from the second lowest lying unoccupied MO) is metal–metal antibonding (Figure 9). In an attempt to understand the reasons for the different electrochemical behaviors of the complexes $Fe_2(CO)_6(RR'C{=}C{=}C{=}CRR')$ as a function of the organic substituent, we have compared the electronic structures of $Fe_2(CO)_6(MeHC{=}C{=}C{=}CHMe)$ (2) and $Fe_2(CO)_6(Me_2C{=}C{=}C{=}CMe_2)$ (3) with that of 1. The $H_2C{=}C{=}C{=}CH_2$, $MeHC{=}C{=}C{=}CHMe$, and $Me_2C{=}C{=}C{=}CMe_2$ ligands interact with the $Fe_2(CO)_6$ fragment in analogous manners, and the interfragment orbital analysis given above is equally appropriate for any of the three complexes. The Fenske–Hall HOMO–LUMO separations are also very similar: 3.70 eV for 1, 3.60 eV for 2, and 3.57 eV for 3.[20] There is no apparent electronic effect to which we can attribute the changes in the electrochemical behavior. However, it seems reasonable that,

(19) Thorn, D. L.; Hoffmann, R. *Inorg. Chem.* **1978**, *17*, 126.

(20) Note that it is the trend in these values that we find significant, not the absolute values themselves.

as a result of Fe–Fe bond weakening, (and, presumably, lengthening) upon occupation of the LUMO, the organic ligand may be forced to alter its conformation in order to maintain effective metal–ligand orbital overlap. Figure 8a,b illustrates that the interactions (39–11) and (38–10) will be sensitive to changes in the metal–metal bond length. As the steric requirements of the butatriene substituents increase, the flexibility of the chain will tend to become less, thus mitigating against complex reduction.

Concluding Remarks

In this study we have shown that the presence of a large organic chain such as butatriene, interacting with the bimetallic $Fe_2(CO)_6$ moiety in a multicentered σ/π fashion, is able to stabilize the electrogenerated anionic species. The LUMO of each butatriene complex is iron–iron antibonding. Thus, on reduction, the metal–metal interaction is weakened. The organic chain serves as a bridge between the metallic centers, altering its conformation but, at the same time, holding the metal atom together. We suggest that, on reoxidation, direct bonding between the two iron atoms can be restored, along with the original conformation of the overall molecule.

In contrast, most of the unbridged $L_xM–ML_x$ complexes[21] (L = CO, C_5H_5), in which such a clasping effect is not present, exhibit a two-electron reduction followed by a complete separation of the metallic moieties:

$$L_xM–ML_x \xrightarrow{2e^-} 2L_xM^-$$

Experimental Section

The $Fe_2(CO)_6$(butatriene) complexes were synthesized according to the literature procedures,[3] as briefly described in the Results and Discussion.

The IR and MS spectra were recorded on Perkin-Elmer 580B and AEI MS 12 instruments, respectively; the ^1H and ^{13}C NMR spectra were obtained on a JEOL GX-270 spectrometer. The ESR spectra were obtained on a Bruker 200 D-SRC instrument, operating at 9.78 GHz (X-band). The electrochemical apparatus was a BAS 100 A (in Siena, Italy) or a PAR 273 instrument (in Torino, Italy). All potentials are referred to the saturated calomel electrode (SCE). Ferrocene was used as an internal standard. Under the actual experimental conditions the $FeCp_2^{0/+}$ couple is located at +0.38 V in MeCN and at +0.49 V in CH_2Cl_2.[21]

The Fenske–Hall[22] quantum-mechanical technique was used to examine the bonding in compounds of formula $Fe_2(CO)_6$(RR′C=C=C=CRR′) (R = R′ = H, **1**; R = Me, R′ = H, **2**; R = R′ = Me, **3**). Atomic coordinates were based on those determined crystallographically for $Fe_2(CO)_6$[μ-bis(biphenylylene)butatriene],[4] but the geometry of each complex was idealized to C_2 symmetry. The structure of the $Fe_2(CO)_6(C_4)$ core of each complex was kept constant throughout the calculations, and only the substituents were altered. Pertinent distances are as follows (Å): Fe–Fe = 2.625, $Fe–C_{CO}$ = 1.74, C–O = 1.15, $C–C_{butatriene}$ = 1.365, C–H = 1.08, $C–C_{Me}$ = 1.52. An atom-numbering scheme is included in Figure 1.

The Fenske–Hall calculations employed single-ζ Slater functions for the 1s and 2s functions of B, C, N, and O. The exponents were obtained by curve-fitting the double-ζ functions of Clementi[23] while maintaining orthogonal functions; the double-ζ functions were used directly for the 2p orbitals. An exponent of 1.16 was used for H. The Fe 1s–3d functions,[24] chosen for the +1 oxidation state, were augmented by 4s and 4p functions with exponents of 2.00.

Acknowledgment. We thank the European Economic Community for financial support. C.E.H. thanks the Royal Society for a 1983 University Research Fellowship; the SERC is acknowledged for a grant (S.M.O.).

Registry No. **1**, 12211-98-2; 1^-, 126821-42-9; 1^{2-}, 126821-46-3; 1^{2+}, 126821-50-9; **2**, 63230-17-1; 2^-, 126821-43-0; 2^{2-}, 126821-47-4; 2^{2+}, 126821-51-0; **3**, 12212-46-3; 3^-, 126821-44-1; 3^{2-}, 126821-48-5; 3^{2+}, 126821-52-1; **4**, 41395-54-4; 4^-, 126821-45-2; 4^{2-}, 126821-49-6; 4^{2+}, 126821-53-2; CH_3CN, 75-05-8; CH_2Cl_2, 75-09-2.

(21) Dessy, R. E.; King, R. B.; Waldrop, N. J. *J. Am. Chem. Soc.* **1966**, *88*, 5117.
(22) Gritzner, G.; Kuta, J. *Pure Appl. Chem.* **1982**, *54*, 1527.
(23) Hall, M. B.; Fenske, R. F. *Inorg. Chem.* **1972**, *11*, 768.
(24) Clementi, E. *J. Chem. Phys.* **1964**, *40*, 1944.
(25) Richardson, J. W.; Nieuwpoort, W. C.; Powell, R. R.; Edgell, W. F. *J. Chem. Phys.* **1962**, *36*, 1057.
(26) Kostic, N. M.; Fenske, R. F. *Organometallics* **1982**, *1*, 974.